A geometry-based comprehensive heat source model for FE thermal simulation of laser directed energy deposition

Ali Zardoshtian^{1,2}, Hamid Jahed², Ehsan Toyserkani^{1,*}

- ¹ Multi Scale Additive Manufacturing Lab, Department of Mechanical and Mechatronics Engineering, University of Waterloo, Waterloo, Ontario, Canada
- ² Fatigue and Stress Analysis Lab, Department of Mechanical and Mechatronics Engineering, University of Waterloo, Waterloo, Ontario, Canada
- * ehsan.toyserkani@uwaterloo.ca

Abstract: Laser Directed Energy Deposition (L-DED) is a distinctive manufacturing process known for its relatively high deposition rate, minimal waste, and ability to make complex geometries. Accurate prediction of the temperature distribution and thermal history during L-DED is crucial for estimating the microstructure, porosity, and mechanical properties of the fabricated parts. However, existing analytical and numerical models often fall short in accuracy due to overlooking the geometrical characteristics and shape of the deposition. To address this issue, a multi-step statistical/numerical analysis workflow is proposed to elucidate the thermal responses in L-DED deposited tracks. First, a data-driven predictive model using statistical methods was used to estimate the deposition geometry based on the key process parameters which are laser power (P), powder feed rate (F), and scanning speed (V). Next, the prediction results were implemented in a dynamic hybrid quiet/inactive elemental control scheme to capture the deposition process. Further, activated elements are subsequently analyzed thermally through a transient 3-D finite element (FE) heat source model accounting for heat flux from conduction, convection, and radiation. The laser beam's energy follows a twodimensional Gaussian distribution, while the heat flux over the actual deposition region, modeled as a quarter-ellipsoid with the predicted geometrical characteristics. This representation captures the actual projection of the laser beam on the deposition. The simulated melt pool depths and temperature showed excellent agreement with experimental measurements for L-DED depositions of Inconel 625 superalloy, exhibiting less than 10% deviation, thereby validating the proposed heat source model.

Keywords: FEA, Statistical Analysis, L-DED Additive Manufacturing, Heat Source Model

1. Introduction

Laser-Directed Energy Deposition (L-DED) is an additive manufacturing technique that fabricates metal components by feeding material, typically powder or wire, directly into a melt pool created by a focused laser beam [1]. To optimize process parameters, reduce costly trial-and-error, and gain insight into temperature distribution, researchers have developed a range of statistical methods based on small-scale experimentations [2], [3] as well as numerical methods, including 3D finite-element and computational fluid dynamics models, to simulate heat transfer, melt-pool dynamics, and microstructure evolution in L-DED [1]. In this study, to accurately simulate thermal histories and predict melt pool geometry, a hybrid statistical-numerical approach is implemented that integrates experimentally validated deposition geometries with a customized moving heat source model. Initially, single-track depositions of Inconel 625 alloy were fabricated using a wide range of process parameters, including laser power, scanning speed, and powder feed rate. The geometrical characteristics of the resulting tracks, specifically height, width, and penetration depth, were precisely measured and used to develop a predictive statistical model. Compared to conventional 3D modelling approaches, this model captures the dependence of deposition geometry on process parameters via empirical functions, and its output is directly employed to define the shape and size of the deposition zone.

2. Methodology

2.1. Statistical modelling & design of experiment

Empirical-statistical modelling was used to study the main process parameters' effects, including the laser power (P), scanning speed (V), and powder feeding rate (F), on the geometrical characteristics of the single-track depositions: the height (h), width (W) and the melt pool's penetration depth to the substrate (b). In that regard, a full factorial design of experiments (DoE) was applied, and the relationships between the deposition geometry and process parameters were described using the following exponential function [4]:

$$y = \left(\frac{P}{\sqrt{N}}\right)^{\alpha} \times \left(\frac{F}{V}\right)^{\beta} \tag{1}$$

Where, α , and β are the constants of the function that can be obtained through the linear regression analysis.

2.2. L-DED processing & Experimental validation

An in-house developed robotic L-DED system (shown in Figure 1 (a)) was used to deposit the DoE's single-tracks with a length of 30 mm on the substrate. During the experiments, the laser spot size was maintained at 1.2 mm and the ranges of the main process parameters namely, laser power, scanning speed, and powder feed rate are 300-700 W, 3-7 mm/s, and 3-7 g/min, respectively. Figure 1(b) schematically shows the L-DED process and the geometrical characteristics (*h*, *W*, and *b*) of the depositions, which were measured for both statistical analysis and validation of the FE thermal model.

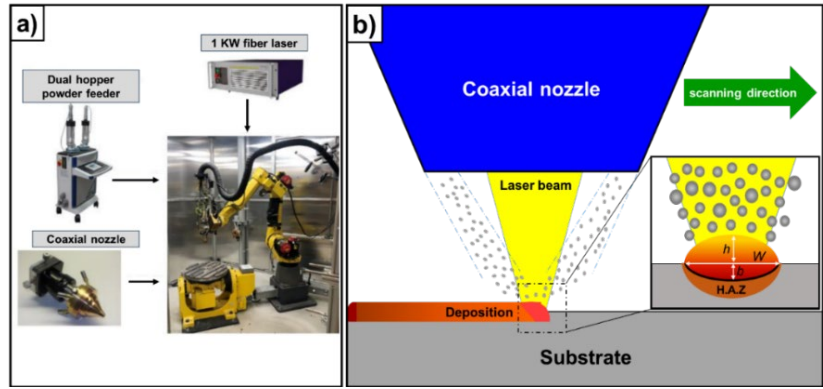


Figure 1. (a) L-DED setup, (b) schematic of the deposition's geometrical characteristics

3. Finite element (FE) modelling

The proposed numerical model for the L-DED process discretizes the continuous laser metal deposition process into a series of sequential simulation steps, each corresponding to a specific segment of the laser path. The commercial FE software Abaqus 2023 was used to simulate the depositions and temperature distribution during the process. To reduce computational effort, the model leveraged the process's geometric symmetry by simulating only half of the substrate and a single-track deposition, as shown in Figure 2. The substrate domain was defined as $5 \times 5 \times 15$ mm, with the deposition track placed on top and measuring $2 \times 2 \times 10$ mm. The simulation employed DC3D8 hexahedral elements.

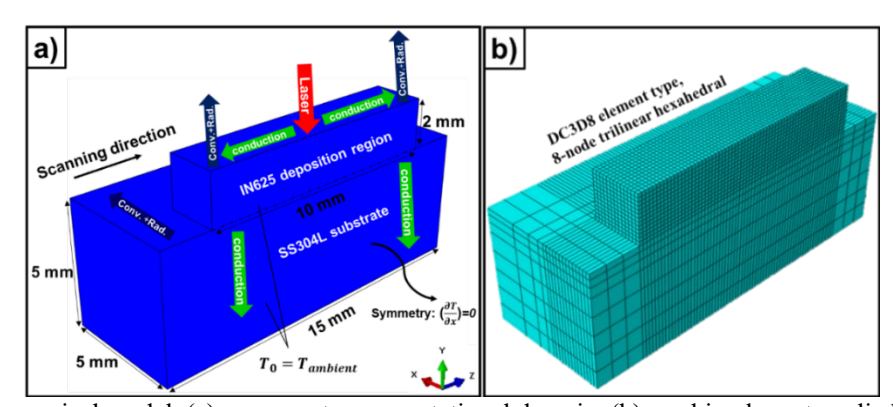


Figure 2. FE numerical model, (a) x-symmetry computational domain, (b) meshing layout applied for the model.

3.1. Material properties, heat transfer governing equation, boundary conditions, and heat source model

The temperature-dependent thermophysical properties of SS304L steel and IN625 superalloy (Table 1) were assigned. The absorption coefficient of 0.6 is assumed for the beam. The thermal conductivity of the materials was multiplied by the constant of 4 for temperatures above the liquidus point (1610 K)[1].

Table 1. Thermophysical properties of IN625 and SS304L						
Material	Thermal conductivity	Specific heat	Density	Liqu.	Solid.	Latent heat of
	(W/m K)	(J/kg K)	(kg/m3)	Temp. (K)	Temp. (K)	fusion (KJ/Kg)
IN625	K _{IN625} =0.014T+7.78	Cp _{IN625} =0.16T+387.1	ρ_{IN625} =-0.8T+8903	1610	1563	227
SS304L	$K_{SS304L} = 0.015T + 9.51$	$Cp_{IN625}=0.14T+455.2$	ρ_{SS304L} =-0.3T+7916	1727	1673	290

The governing equation of heat transfer can be found in [1]. A heat source with a cylindrical-Gaussian shape was applied. The cylindrical heat source model and its 2D Gaussian intensity distribution follow the equations below:

$$I(x,y) = q_0 \cdot \exp\left[-2\frac{x^2 + y^2}{r^2}\right]$$
 (2)

While,

$$\eta. P/V = \int_{-\infty}^{\infty} \int_{-\infty}^{\infty} q_0 \cdot \exp\left[-2\frac{x^2 + y^2}{r^2}\right] dx dy$$
 (3)

I(x, y), q_0 , r, η , P, V, h are the heat intensity distribution, maximum value of heat intensity, radius of the laser beam, laser's absorptivity coefficient, laser power, the volume of the irradiated region in the deposition, and the height.

3.2. Outline of the statistical-numerical approach & Material deposition modelling

The flowchart in Figure 3(a) outlines the comprehensive workflow employed in this work for finite element (FE) thermal modelling of the L-DED process. At the core of the framework is the implementation of material deposition, thermal loads, and convective and radiative heat interactions, which are facilitated through USDFLD, DFLUX, and FILM user-defined subroutines in Fortran. In this study, for material deposition modelling, the hybrid inactive/quiet element method is proposed. As shown in Figure 3(b), in this approach, elements of the deposition region are initially inactive, then they are switched to active on a step-by-step basis. During the thermal analysis, the USFLD subroutine changes the artificial material properties of the quiet elements to their real ones for the areas to be scanned by the heat source.

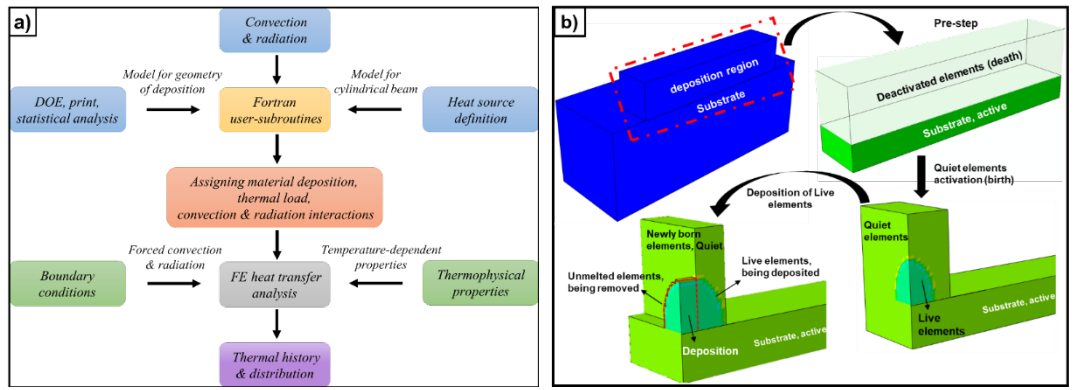


Figure 3. (a) Outline of the statistical-numerical method; (b) Hybrid inactive/quiet element activation approach.

4. Results and discussions

4.1. Statistical analysis of geometrical characteristics

Figure 4 illustrates the empirical correlation between the geometrical characteristics of the deposited track versus the combined process parameters. As shown in Figure 4(a), the height of the deposition increases with rising laser power and decreasing scanning speed, which results in greater heat input per unit length. A higher powder feed rate also contributes to an increased track height due to more material for melting. Figure 4(b) reveals that while higher laser power promotes wider melt pools, an increased powder feed rate appears to have a counteracting effect. Figure 4(c) confirms a positive correlation between energy input and melt pool penetration depth, due to enhanced substrate melting.

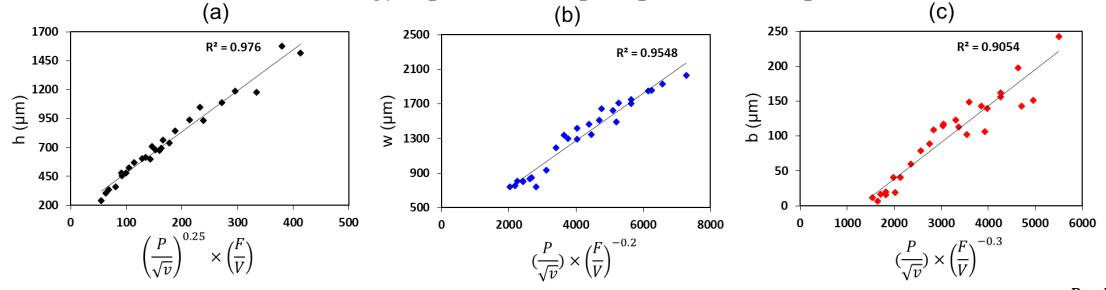


Figure 4. The correlation of a) height, b) width, c) depth of depositions with the process parameters $(\frac{P}{\sqrt{\nu}}, \frac{F}{V})$

4.2. Comparison Between Experimental Deposition Profile and Simulated Thermal Field

Figure 5 presents a direct comparison between experimentally measured geometrical characteristics of deposition and FE predicted temperature fields under various parameters. Across different process parameters, the numerical predictions closely match the experimental measurements. It is important to note that the top surface of the simulated deposition appears slightly cooler than the central regions. This is due to the outer corner nodes of the recently deposited elements

initially retaining artificial material properties, while only the inner nodes of the same elements are assigned the actual material properties upon activation. As a result, these corner nodes exhibit lower temperatures.

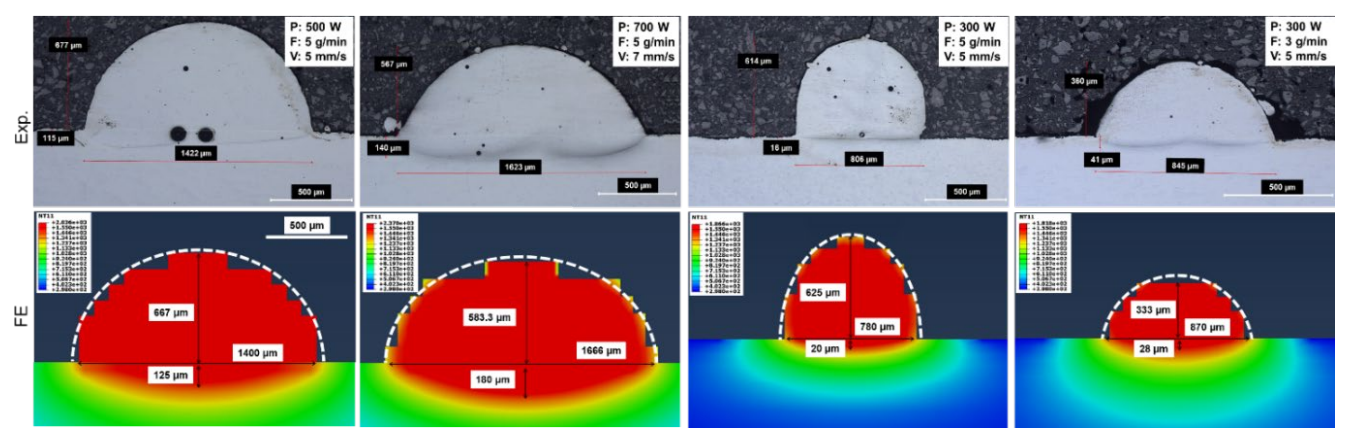


Figure 5. Geometrical characteristics of depositions in experiments vs. FE results.

4.3. Effect of process parameters on the deposition's dimensions

Figure 6 compares the experimentally measured and numerically simulated geometrical characteristics under four different sets of process parameters. Each plot demonstrates a strong correlation between FE predictions and experimental results, with both datasets following a consistent trend across different parameter ranges. Together, these results emphasize that both $(\frac{P}{\sqrt{V}})$ and $(\frac{F}{V})$ are critical parameters governing deposition's geometry in L-DED.

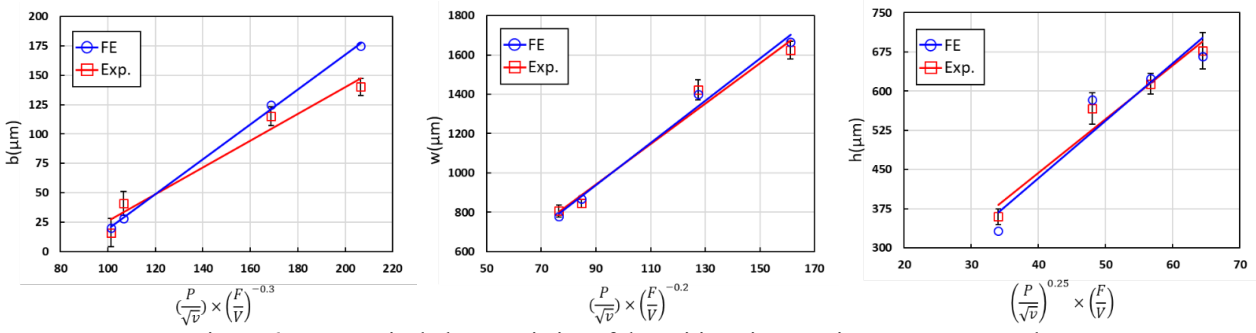


Figure 6. Geometrical characteristics of depositions in experiments vs. FE results.

5. Summary

This study presents a hybrid statistical-numerical finite element (FE) thermal modelling framework for simulating L-DED process. The methodology integrated empirical-statistical modelling with a customized cylindrical-Gaussian heat source implemented in Abaqus via user subroutines. The main findings are summarized below:

- 1. The deposited single-track geometrical characteristics, height (h), width (W), and penetration depth (b), have a strong correlation with combined efficient process parameters $(\frac{P}{\sqrt{V}})$ and $(\frac{F}{V})$ with $R^2 > 90\%$.
- 2. A quarter-ellipsoidal thermal model was developed, and the hybrid inactive/quiet element activation strategy was used to simulate material deposition. The model was validated by comparing the simulated geometrical characteristics with experimental measurements.

Future studies could build upon this by deriving cooling rates and thermal gradients to establish correlations with microstructural evolution within the deposited material.

6. References

- [1] M. Gouge and P. Michaleris, Thermo-mechanical modeling of additive manufacturing. Butterworth-Heinemann, 2017.
- [2] A. Zardoshtian, M. Ansari, R. Esmaeilzadeh, A. Keshavarzkermani, H. Jahed, and E. Toyserkani, "Laser-directed energy deposition of CuCrZr alloy: from statistical process parameter optimization to microstructural analysis," The International Journal of Advanced Manufacturing Technology, vol. 126, no. 9, pp. 4407–4418, 2023.
- [3] A. Zardoshtian, R. Esmaeilizadeh, M. Ansari, M. K. Keshavarz, H. Jahed, and E. Toyserkani, "On the Processability and Microstructural Evolution of CuCrZr in Multilayer Laser-Directed Energy Deposition Additive Manufacturing via Statistical and Experimental Methods," 2023. doi: 10.3390/jmmp7040151.
- [4] R. Ghanavati, H. Naffakh-Moosavy, M. Moradi, and M. Eshraghi, "Printability and microstructure of directed energy deposited SS316l-IN718 multi-material: numerical modeling and experimental analysis," Sci Rep, vol. 12, no. 1, pp. 1–16, 2022, doi: 10.1038/s41598-022-21077-8.